

Supporting Information

Manipulation of Solubility and Interstitial Defects for Improving Thermoelectric SnTe Alloys

Jing Tang¹, Bo Gao¹, Siqi Lin¹, Xiao wang¹, Xinyue Zhang¹, Fen Xiong², Wen Li¹, Yue Chen² and Yanzhong Pei^{*,1}

¹Interdisciplinary Materials Research Center, School of Materials Science and Engineering, Tongji Univ., 4800 Caoan Rd.,

Shanghai 201804, China.

²Department of Mechanical Engineering, The University of Hong Kong, Pokfulam Road, Hong Kong SAR, China

*Email: yanzhong@tongji.edu.cn

Details on materials and methods

Polycrystalline $\text{Sn}_{0.95-x+\delta}\text{Ge}_{0.05}\text{Cd}_x\text{Te}$ and $\text{Sn}_{0.95-x+\delta}\text{Ge}_{0.05}\text{Cd}_x\text{Te}(\text{Cu}_2\text{Te})_{0.05}$ with x up to 0.24, δ up to 0.06, were synthesized by melting the stoichiometric amounts of high purity elements Sn(99.99%), Te(99.99%), Ge(99.999%), Cd(99.999%), Cu(99.99%) at 1223 K for 6 hours, quenching in cold water. The resulting ingots were hand ground into fine powder for X-ray diffraction (XRD). The samples are hot pressed by an induction heating hot press system¹ at 900 K for 45 mins under a uniaxial pressure of ~60 MPa for $\text{Sn}_{0.95-x+\delta}\text{Ge}_{0.05}\text{Cd}_x\text{Te}$ and ~65Mpa for $\text{Sn}_{0.95-x+\delta}\text{Ge}_{0.05}\text{Cd}_x\text{Te}(\text{Cu}_2\text{Te})_{0.05}$. The obtained dense samples (>98% of the theoretical density) are ~12 mm in diameter and ~1.5 mm in thickness. Scanning electronic microscopy (SEM) instrument equipped with an energy dispersive spectrometer (EDS) apparatus was used for characterizing the microstructure and inferring the solubility of CdTe in SnTe.

The electric transport properties including resistivity, Seebeck coefficient and Hall coefficient of pellet samples are measured in the temperature range of 300K to 900K under a helium atmosphere. The Seebeck coefficient was calculated by the slope of the thermopower vs. temperature gradients within 0~5 K². The resistivity and Hall coefficient (R_H) were measured by the van der Pauw technique under a reversible magnetic field of 1.5 T. Both the seebeck coefficient and resistivity are measured during heating and cooling.

The thermal conductivity was determined by $\kappa=dC_pD$, where d is the density measured using the mass and geometric volume of the pellet. In order to obtain the Thermal diffusivity (D), a laser flash technique with the Netzsch LFA457 system was used. Similar with other IV-VI semiconductors such as PbTe, the heat capacity was determined by $C_p(k_B/\text{atom})=[3.07+0.00047(T/K-300)]^{3-10}$, where T is the absolute temperature. The measurement uncertainty for S , σ and κ is about 5%. Sound velocities were measured using an ultrasonic pulse-receiver (Olympus-NDT) equipped with an oscilloscope (Keysight) and average sound velocities are calculated by longitudinal and transverse sound velocities measured.

First-principles calculations were performed based on density functional theory (DFT) as implemented in Vienna Ab-initio Simulation Package (VASP)¹¹. The generalized gradient approximation of Perdew, Burke, and Ernzerhof¹² was used to calculate the exchange-correlation energy. A cutoff energy of 450 eV for the plane wave basis and a convergence criterion of 1×10^{-5} eV were applied in all calculations. Γ -centered Monkhorst-Pack $4\times 4\times 4$ k -points were applied to mesh the Brillouin zone. A $3\times 3\times 3$ rock-salt supercell, which contains 54 atoms, was constructed to simulate SnTe-alloys. We have substituted one, three or five Sn atoms in the supercell with Cd atoms, corresponding to alloying concentrations of approximately 4%, 11% or 19%, respectively. To simulate the atomic distributions in SnTe alloys, special quasi-random structures were generated using USPEX¹³ by minimizing the structural orders. The effects of spin-orbit coupling (SOC) have also been included in the DFT calculations.

To investigate the effect of Ge on the miscibility of SnTe and CdTe, the energy of mixing is calculated according to the following equation

$$\Delta E = E_{\text{Sn}_{1-x-y}\text{Ge}_x\text{Cd}_y\text{Te}} - E_{\text{Sn}_{1-x-y}\text{Ge}_x\text{Te}_{1-y}} - E_{\text{Cd}_y\text{Te}_y}$$

In the SnTe supercell which contains 54 atoms, nine Sn atoms with Cd have been substituted, corresponding to a Cd concentration $y\sim 33\%$. A Ge alloying concentration $x\sim 7.4\%$ is also been considered by substituting two Sn atoms in the supercell. Based on DFT calculations, the energies of mixing are equal to 59.2 meV/atom and 58.2 meV/atom before and after Ge alloying, respectively. The results suggest that Ge alloying increases the miscibility of SnTe and CdTe.

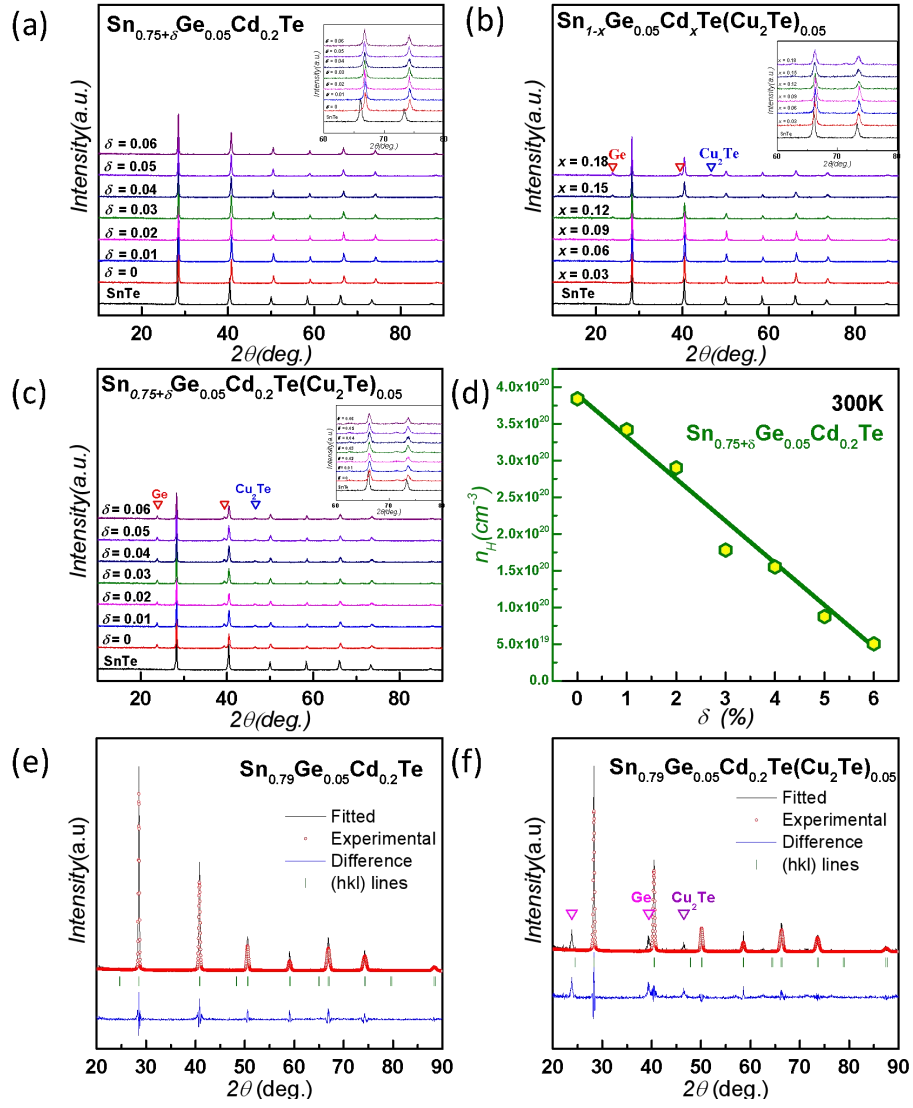
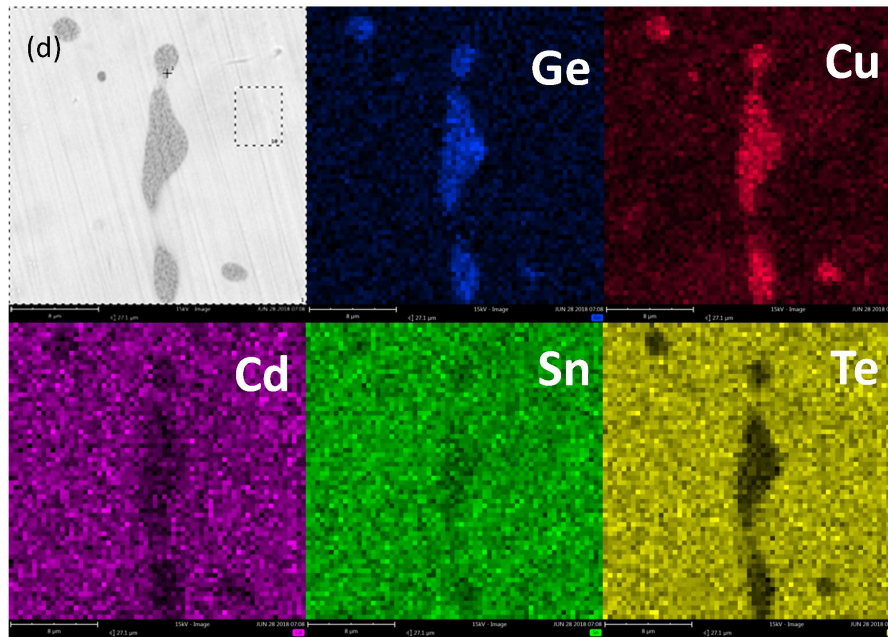
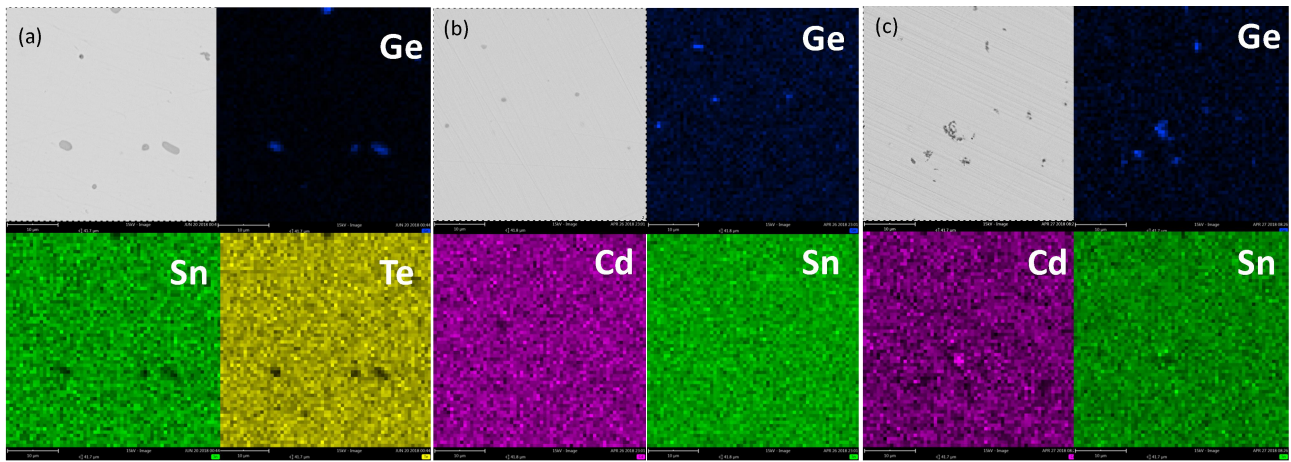
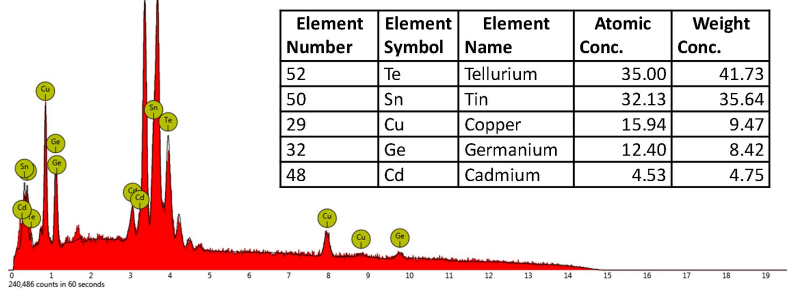


Figure S1. XRD patterns for $\text{Sn}_{0.75+\delta}\text{Ge}_{0.05}\text{Cd}_{0.2}\text{Te}$ (a), $\text{Sn}_{1-x}\text{Ge}_{0.05}\text{Cd}_x\text{Te}(\text{Cu}_2\text{Te})_{0.05}$ (b) and $\text{Sn}_{0.75+\delta}\text{Ge}_{0.05}\text{Cd}_{0.2}\text{Te}(\text{Cu}_2\text{Te})_{0.05}$ (c), as well as room temperature Hall carrier concentration for $\text{Sn}_{0.75+\delta}\text{Ge}_{0.05}\text{Cd}_{0.2}\text{Te}$ (d) and XRD Rietveld refinements to the rock-salt phase in $\text{Sn}_{0.79}\text{Ge}_{0.05}\text{Cd}_{0.2}\text{Te}$ (e) and $\text{Sn}_{0.79}\text{Ge}_{0.05}\text{Cd}_{0.2}\text{Te}(\text{Cu}_2\text{Te})_{0.05}$ (f).



(e) **Elemental compositions for precipitate phase**



(f) **Elemental compositions for matrix phase**

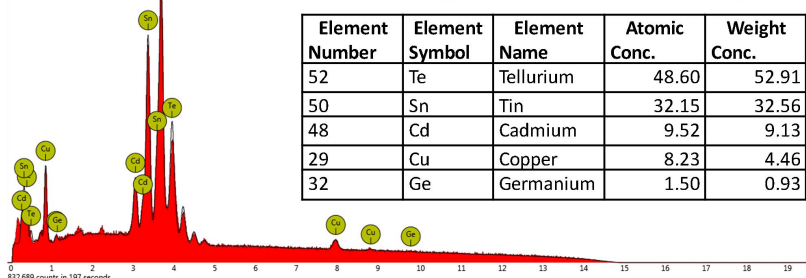


Figure S2. SEM images with composition mappings (a, b, c, d) by EDS for $\text{Sn}_{0.95}\text{Ge}_{0.05}\text{Te}$ (a) $\text{Sn}_{0.75}\text{Ge}_{0.05}\text{Cd}_{0.2}\text{Te}$ (b) $\text{Sn}_{0.79}\text{Ge}_{0.05}\text{Cd}_{0.2}\text{Te}$ (c) and $\text{Sn}_{0.79}\text{Ge}_{0.05}\text{Cd}_{0.2}\text{Te}(\text{Cu}_2\text{Te})_{0.05}$ (d), and the compositions for precipitates (e) and for matrix (f) in $\text{Sn}_{0.79}\text{Ge}_{0.05}\text{Cd}_{0.2}\text{Te}(\text{Cu}_2\text{Te})_{0.05}$.

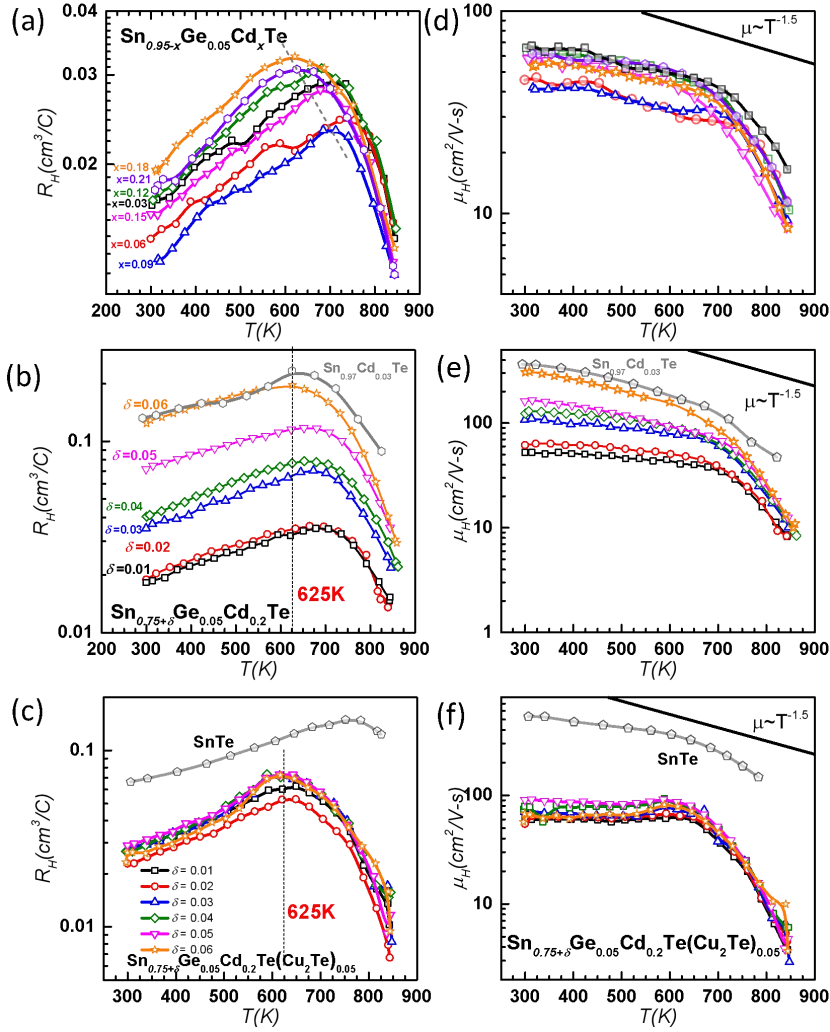


Figure S3. Temperature-dependent Hall coefficient (a, b, c) and Hall mobility (d, e, f) for $\text{Sn}_{0.95-x}\text{Ge}_{0.05}\text{Cd}_x\text{Te}$ (a, d), $\text{Sn}_{0.75+\delta}\text{Ge}_{0.05}\text{Cd}_{0.2}\text{Te}$ (b, e) and $\text{Sn}_{0.75+\delta}\text{Ge}_{0.05}\text{Cd}_{0.2}\text{Te}(\text{Cu}_2\text{Te})_{0.05}$ (c, f), with a comparison to those of $\text{Sn}_{0.97}\text{Cd}_{0.03}\text{Te}^{14}$ and pristine SnTe^{15} .

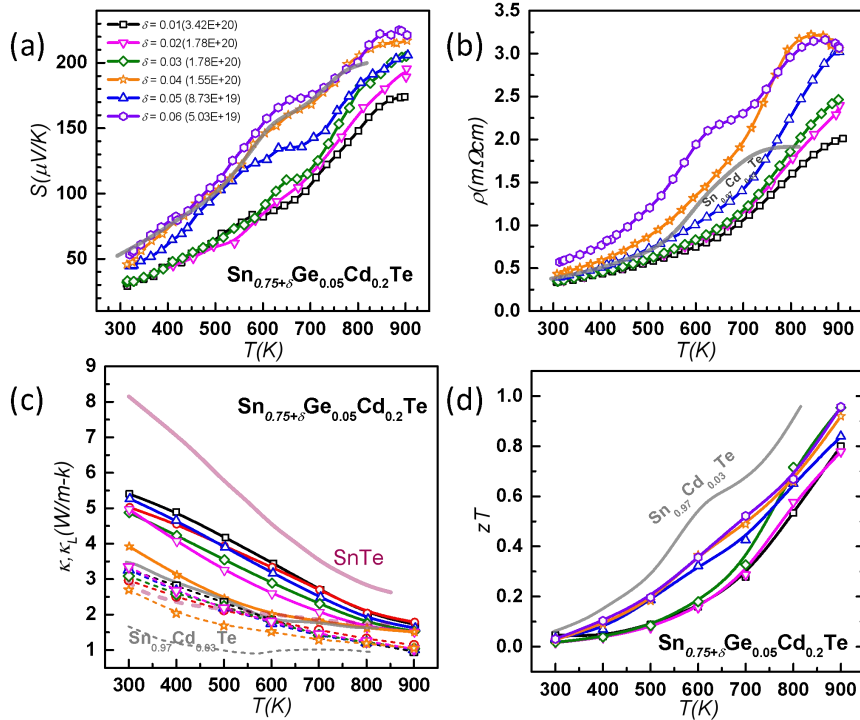


Figure S4. Temperature-dependent Seebeck coefficient (a), resistivity (b), total and lattice thermal conductivity (c) and thermoelectric figure of merit (d) for $\text{Sn}_{0.75+\delta}\text{Ge}_{0.05}\text{Cd}_{0.2}\text{Te}$ with a comparison to those of $\text{Sn}_{0.97}\text{Cd}_{0.03}\text{Te}^{14}$ and pristine SnTe^{15} .

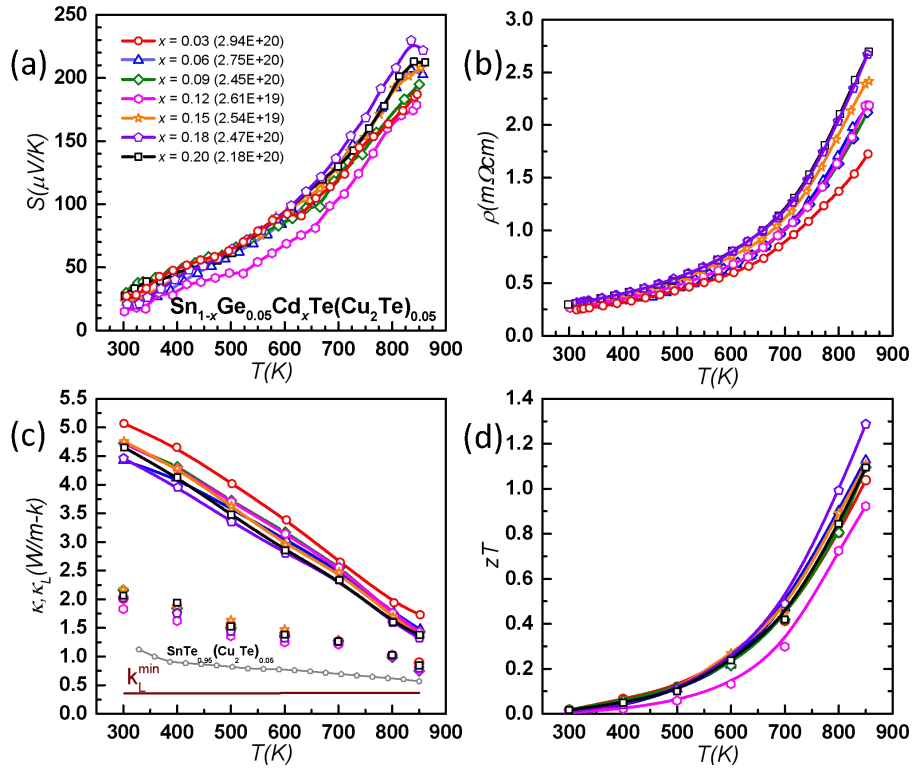


Figure S5. Temperature-dependent Seebeck coefficient (a), resistivity (b), total and lattice thermal conductivity (c) and thermoelectric figure of merit (d) for $\text{Sn}_{1-x}\text{Ge}_{0.05}\text{Cd}_x\text{Te}(\text{Cu}_2\text{Te})_{0.05}$, with a comparison to those of $\text{SnTe}_{0.95}(\text{Cu}_2\text{Te})_{0.05}$ ¹⁵.

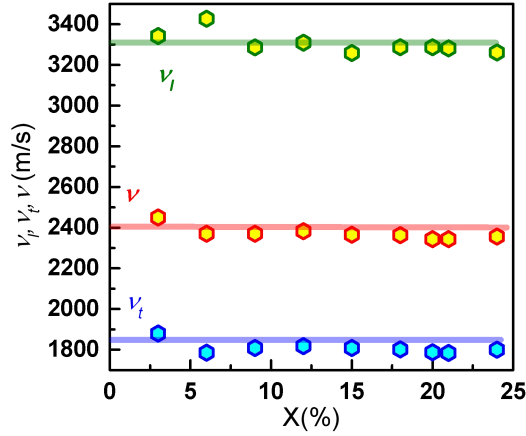


Figure S6. Longitudinal (v_l), transverse (v_t) and average (v) sound velocities at room temperature for $\text{Sn}_{0.95-x}\text{Ge}_{0.05}\text{Cd}_x\text{Te}$.

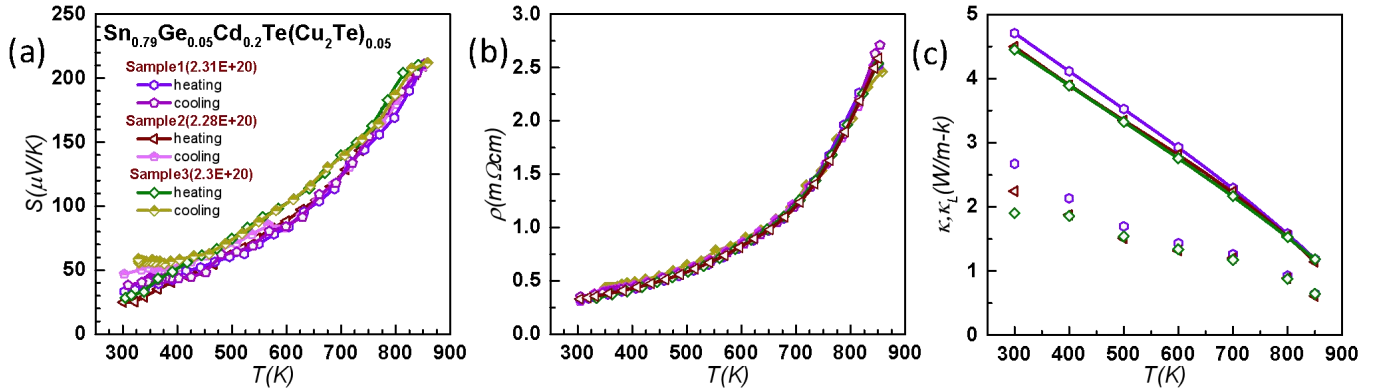


Figure S7. Temperature-dependent Seebeck coefficient (a), resistivity (b), total and lattice thermal conductivity (c) for $\text{Sn}_{0.79}\text{Cd}_{0.2}\text{Ge}_{0.05}\text{Te}(\text{Cu}_2\text{Te})_{0.05}$ synthesized and/or measured repeatedly.

References

- (1) LaLonde, A. D.; Ikeda, T.; Snyder, G. J. Rapid Consolidation of Powdered Materials by Induction Hot Pressing. *Rev. Sci. Instrum.* **2011**, *82*, 025104.
- (2) Zhou, Z.; Uher, C. Apparatus for Seebeck Coefficient and Electrical Resistivity Measurements of Bulk Thermoelectric Materials at High Temperature. *Rev. Sci. Instrum.* **2005**, *76*, 023901.
- (3) Pei, Y.; Wang, H.; Snyder, G. J. Band Engineering of Thermoelectric Materials. *Adv. Mater.* **2012**, *24*, 6125–6135.
- (4) Pei, Y.; Shi, X.; LaLonde, A.; Wang, H.; Chen, L.; Snyder, G. J. Convergence of Electronic Bands for High Performance Bulk Thermoelectrics. *Nature* **2011**, *473*, 66-69.
- (5) Lin, S. Q.; Li, W.; Chen, Z. W.; Shen, J. W.; Ge, B. H.; Pei, Y. Z. Tellurium as a High-Performance Elemental Thermoelectric. *Nat. Commun.* **2016**, *7*, 10287.
- (6) Heremans, J. P.; Jovovic, V.; Toberer, E. S.; Saramat, A.; Kurosaki, K.; Charoenphakdee, A.; Yamanaka, S.; Snyder, G. J. Enhancement of Thermoelectric Efficiency in PbTe by Distortion of the Electronic Density of States. *Science* **2008**, *321*, 554-557.
- (7) Pei, Y.; LaLonde, A. D.; Heinz, N. A.; Snyder, G. J. High Thermoelectric Figure of Merit in PbTe Alloys Demonstrated in PbTe–CdTe. *Adv. Energy Mater.* **2012**, *2* (6), 670-675.
- (8) Pei, Y.; LaLonde, A. D.; Wang, H.; Snyder, G. J. Low Effective Mass Leading to High Thermoelectric Performance. *Energy Environ. Sci.* **2012**, *5*, 7963-7969.
- (9) Pei, Y.; LaLonde, A.; Iwanaga, S.; Snyder, G. J. High Thermoelectric Figure of Merit in Heavy-Hole Dominated PbTe. *Energy Environ. Sci.* **2011**, *4*, 2085–2089.
- (10) Pei, Y.; May, A. F.; Snyder, G. J. Self-Tuning the Carrier Concentration of PbTe/Ag₂Te Composites with Excess Ag for High Thermoelectric Performance. *Adv. Energy Mater.* **2011**, *1*, 291-296.
- (11) Kresse G, F. J. Efficient Iterative Schemes for Ab Initio Total-Energy Calculations Using a Plane-Wave Basis Set. *Phys. Rev. B* **1996**, *54*, 11169-11186.
- (12) Perdew JP, B. K., Ernzerhof M. Generalized Gradient Approximation Made Simple. *Phys. Rev. Lett.* **1996**, *77*, 3865-3868.
- (13) Oganov AR, V. M. How to Quantify Energy Landscapes of Solids. *J. Chem. Phys.* **2009**, *130*, DOI: 10.1063/1061.3079326.
- (14) Tan, G.; Zhao, L. D.; Shi, F.; Doak, J. W.; Lo, S. H.; Sun, H.; Wolverton, C.; Dravid, V. P.; Uher, C.; Kanatzidis, M. G. High Thermoelectric Performance of p-Type SnTe via a Synergistic Band Engineering and Nanostructuring Approach. *J. Am. Chem. Soc.* **2014**, *136*, 7006-7017.
- (15) Pei, Y. Z.; Zheng, L. L.; Li, W.; Lin, S. Q.; Chen, Z. W.; Wang, Y. Y.; Xu, X. F.; Yu, H. L.; Chen, Y.; Ge, B. H. Interstitial Point Defect Scattering Contributing to High Thermoelectric Performance in SnTe. *Adv. Electron. Mater.* **2016**, *2*, 1600019.